Liquid Crystals

Publication details, including instructions for authors and subscription information:
http://www.informaworld.com/smpp/title~content=t713926090

Novel glass-forming liquid crystals V. Nematic and chiral-nematic systems with an elevated glass transition temperature

Fred Y. Fan[a]; John C. Mastrangelo[a]; Dimitris Katsis[a]; Shaw H. Chen[a]
[a] Center for Optoelectronics and Imaging, University of Rochester, 240 East River Road, Rochester, New York 14623-1212, USA,

To cite this Article Fan, Fred Y. , Mastrangelo, John C. , Katsis, Dimitris and Chen, Shaw H.(2000) 'Novel glass-forming liquid crystals V. Nematic and chiral-nematic systems with an elevated glass transition temperature', Liquid Crystals, 27: 9, 1239 — 1248

To link to this Article: DOI: 10.1080/02678290050122105

URL: http://dx.doi.org/10.1080/02678290050122105

LIQUID CRYSTALS, 2000, VOL. 27, NO. 9, 1239–1248

Novel glass-forming liquid crystals V. Nematic and chiral-nematic systems with an elevated glass transition temperature

FRED Y. FAN, JOHN C. MASTRANGELO, DIMITRIS KATSIS,
SHAW H. CHEN*
Center for Optoelectronics and Imaging, University of Rochester,
240 East River Road, Rochester, New York 14623-1212, USA

and THOMAS N. BLANTON
Analytical Technology Division, Kodak Research Laboratories B82A,
Eastman Kodak Company, Rochester, New York 14650-2106, USA

(*Received 2 September 1999; in final form 10 March 2000; accepted 16 March 2000*)

The formerly implemented molecular design concept behind glass-forming liquid crystals (gLCs) was generalized by increasing the volume of the non-mesogenic central core, with an attendant increase in the number of nematic pendants, using 5-hydroxyisophthalic acid as the bridging unit. New nematic gLCs were synthesized and characterized, showing an elevation in T_g by 30 to 40°C with no definite trend in T_c over the benzene, *cis,cis*-cyclohexane, and *exo,endo*-bicyclo[2.2.2]oct-7-ene base cores. The *exo,exo*-configured gLC showed a higher T_g and a higher T_c than the *exo,endo*-counterpart. Morphological characterization with X-ray diffractometry revealed the non-crystalline nature of pristine samples and the morphological stability of thermally processed gLC films against recrystallization for six months. Nematic gLC films were prepared for characterization by FTIR linear dichroism, resulting in an orientational order parameter in the range 0.52 to 0.63. A chiral-nematic gLC derived from *exo,exo*-bicyclo[2.2.2.]oct-7-ene also showed an elevation in T_g by 10 to 20°C over the cyclohexane-based systems reported previously. With (*S*)-(−)-1-phenylethylamine as the chiral moiety, the left-handed, chiral-nematic gLC film yielded a selective reflection band centred around 375 nm. Tunability of selective reflection from the UV to visible region was demonstrated by mixing the chiral-nematic and nematic gLCs at varying ratios.

1. Introduction

Liquid crystallinity is a consequence of spontaneous molecular self-assembly into a uniaxial, lamellar, helical, or columnar arrangement on a macroscopic scale. Because of their unique optical properties, liquid crystals are potentially useful as optical, photonic and optoelectronic devices [1]. In some of these applications, such as liquid crystal displays, the material functions in the fluid state where an applied field induces molecular reorientation with a response time on the order of milliseconds. With judiciously designed structural moieties, liquid crystals may also function in the solid state via a photonic or electronic stimulus with a much shorter response time. In addition, liquid crystals can be employed as passive devices in which no switching is involved. With the exception of applications in which molecular reorientation with an applied field is the basis, vitrified liquid crystals with an elevated glass transition temperature, T_g, offer long term mesomorphic stability as well as environmental durability. Whereas glass formation appears to be a privilege of liquid crystalline polymers, their generally high melt viscosity presents a major challenge to processing into large area thin films. To combine ease of material processing with glass-forming ability in discrete molecular systems, extensive efforts have been made over the last two decades [2–5] to develop glass-forming liquid crystals (gLCs) with well defined structures having low to medium molecular weights. Applications that have been explored with various gLCs include: optical data storage [6, 7], optical non-linearity [8, 9], photochromism [10], tunable filters for optical communication [11], and viewing angle compensation for displays [12].

To furnish morphologically stable gLCs, we have successfully implemented a general molecular design approach in which mesogenic and chiral groups are

---

*Author for correspondence; e-mail: shch@lle.rochester.edu

Liquid Crystals ISSN 0267-8292 print/ISSN 1366-5855 online © 2000 Taylor & Francis Ltd
http://www.tandf.co.uk/journals

chemically bonded to a central core, such as adamantane, bicyclo-octene, cyclohexane, and cubane [13–15]. The principle is to have the two structural elements impose volume exclusion on each other as a way to prevent spontaneous crystallization. The pendant group and the central core, as separate entities, are crystalline with a high melting point, but the hybrid system readily forms a glass on cooling. Various gLCs have been synthesized which exhibit nematic, smectic, and cholesteric mesophases with a T_g generally between 60 and 80°C and a clearing temperature, T_c, beyond 250°C [16]. In comparison with polymer analogues, this novel material class is characterized by a low melt viscosity [17], a short and uniform mechanical relaxation time [17], and an expedited annihilation of disclinations [18], resulting in nearly defect-free films. Furthermore, gLCs were found to emulate high polymers in terms of morphological stability against thermally-activated recrystallization [19]. All these desirable properties combine to render gLCs favourable over liquid crystalline polymers for practical applications. Specifically, optical quality films were prepared for selective reflection and circular polarization [20] as well as circularly polarized photoluminescence [21]. The present work was motivated by a desire to elevate T_g to and beyond 100°C by increasing the volume of the non-mesogenic central core and the number of mesogenic pendants per gLC molecule.

2. Experimental

2.1. *Reagents and chemicals*

All chemicals, reagents, and solvents were used as received from Aldrich Chemical Company or VWR Scientific with the following exceptions. Tetrahydrofuran (99%) was dried by heating at reflux over sodium in the presence of benzophenone until blue, then distilled for use. Silica gel 60 (EM Science, 230–400 mesh) was used for liquid chromatography.

2.2. *Material synthesis*

Synthesis and purification of intermediates and final products were carried out following schemes 1, 2 and 3. Experimental procedures are described below.

2.2.1. *Cis, cis-cyclohexane-1,3,5-tricarboxylic acid, tris{3-[6-′(4-cyanophenyl)-2′-naphthyloxy]-1-propyl ester} (**I**)*

The synthesis and purification of this nematic gLC has been reported previously [16].

2.2.2. *1-t-Butyldimethylsilyloxy-3,5-benzenedicarboxylic acid (**a**)*

5-Hydroxyisophthalic acid (9.11 g, 50.0 mmol) and *t*-butyldimethylsilyl chloride (25.2 g, 167 mmol) were dissolved in anhydrous *N*,*N*-dimethylformamide (DMF) (55 ml). Upon adding imidazole (20.4 g, 300 mmol), the solution was stirred overnight before shaking with diethyl ether (200 ml) and water (600 ml). The organic layer was reduced in volume by evaporation to a clear oil, which was mixed with tetrahydrofuran (THF) (45 ml), water (30 ml), and glacial acetic acid (30 ml), and acidified with 37% aqueous HCl. The reaction mixture was stirred for 2 h. After evaporating the THF, the solution was shaken with CH_2Cl_2 (200 ml) and water (200 ml). The organic layer was washed twice with water (200 ml each), and the insoluble product was collected by filtration. Additional product was collected by washing with water the solid residue from evaporation of the solvent. A total of 10.1 g (68%) of compound **a** was obtained; its structure was validated by proton NMR spectroscopy.

2.2.3. *2-(3′-Hydroxy-1′-propyloxy)-6-(4-cyanophenyl)-naphthalene (**b**)*

The synthesis and purification of this nematic precursor has been reported previously [16].

2.2.4. *1-t-Butyldimethylsilyloxy-3,5-benzenedicarboxylic acid, bis{3-[6′-(4-cyanophenyl)-2′-naphthyloxy]-1-propyl ester} (**c**)*

Intermediate **a** (1.80 g, 6.07 mmol), intermediate **b** (3.63 g, 12.0 mmol), and triphenylphosphine (3.29 g, 12.6 mmol) were dissolved in anhydrous THF (80 ml). After addition of diethylazodicarboxylate, DEADC, (2.1 ml, 13.3 mmol), the solution was stirred overnight. The solid residue resulting from evaporation to dryness was mixed with CH_2Cl_2, and the insolubles were filtered off. The crude product in the filtrate was purified by column chromatography on silica gel with CH_2Cl_2 as the eluent to obtain compound **c** in 3.49 g (67%) yield; its structure was validated by proton NMR spectroscopy.

2.2.5. *1-Hydroxy-3,5-benzenedicarboxylic acid, bis{3-[6′-(4-cyanophenyl)-2′-naphthyloxy]-1-propyl ester} (**d**)*

Intermediate **c** (3.48 g, 4.0 mmol) was dissolved in THF (30 ml) and acetone (5 ml) at room temperature. The solution was then chilled in an ice water bath. Tetrabutylammonium fluoride solution (1M, 5 ml, 5.0 mmol) [22] was added over 15 min with subsequent stirring for 30 min. The reaction was quenched with ammonium chloride (0.78 g, 14.5 mmol) in water (10 ml). After stirring for 10 min, the solution was shaken with CH_2Cl_2 (200 ml) and water (200 ml). The volume of the organic layer was reduced to 40 ml by evaporation. The solid product in 2.08 g (66%) yield was collected by filtration and its structure validated by proton NMR spectroscopy.

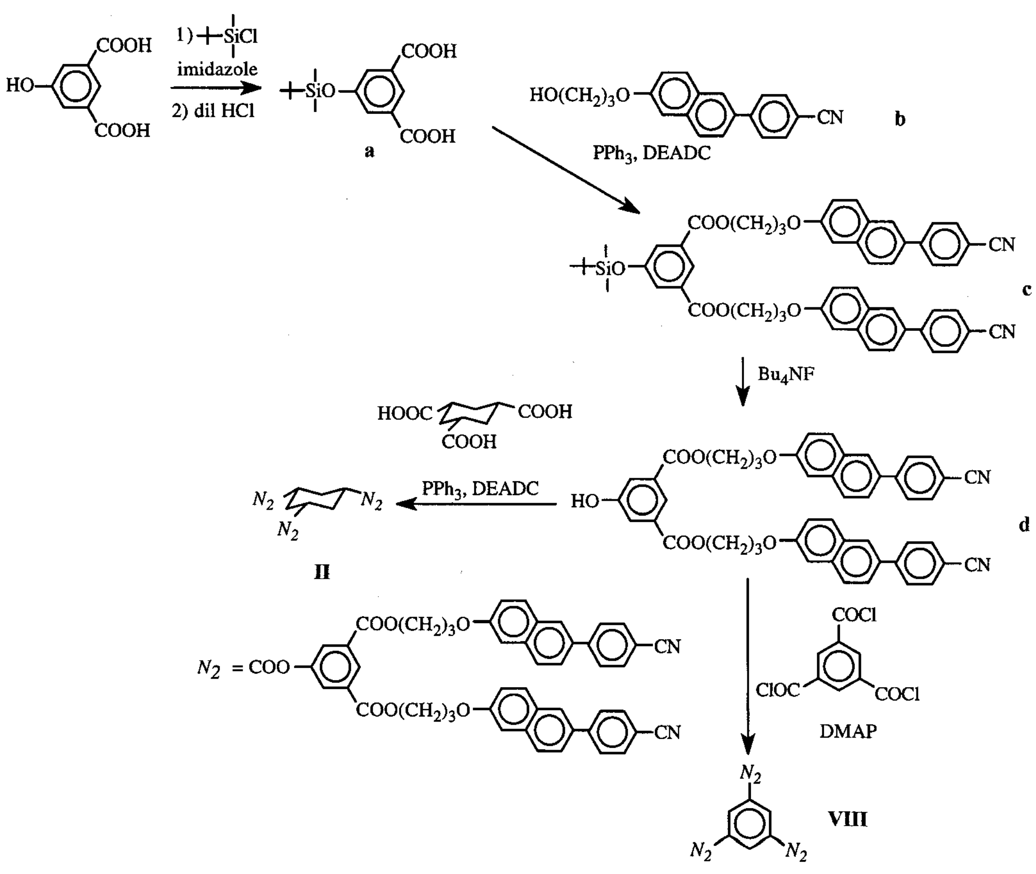

Scheme 1.

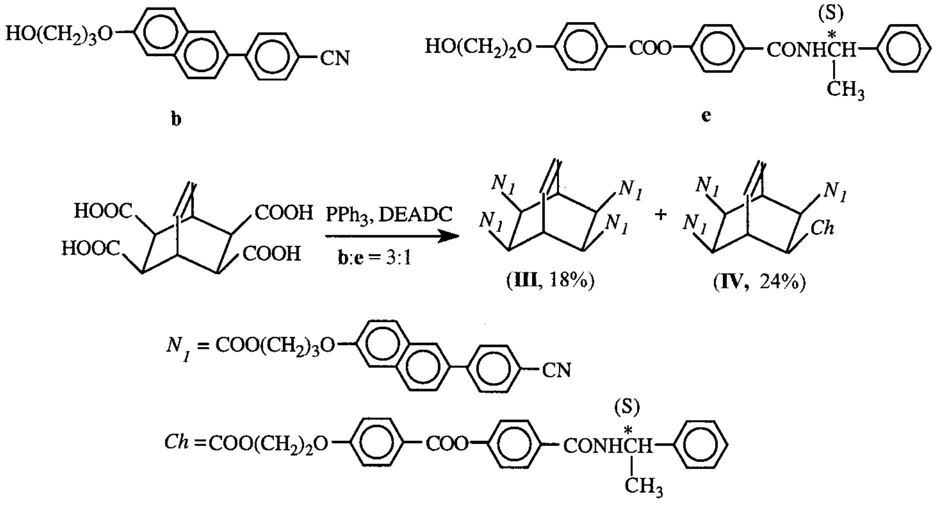

Scheme 2.

2.2.6. *Cis, cis-cyclohexane-1,3,5-tricarboxylic acid, tris{3,5-bis{3-[6'-(4-cyanophenyl)-2'-naphthyloxy]-1-propyloxycarbonyl}phenyl ester} (**II**)*

Intermediate **d** (2.05 g, 2.63 mmol), *cis,cis*-1,3,5-cyclohexanetricarboxylic acid (0.19 g, 8.7 mmol), and triphenylphosphine (0.74 g, 2.83 mmol) were dissolved in anhydrous THF (20 ml) and anhydrous DMF (10 ml). DEADC (0.45 ml, 2.85 mmol) was added to the solution over 5 min, and the reaction mixture was stirred for 2 days. After reducing the volume by evaporation, the reaction mixture was shaken with CH_2Cl_2 (100 ml) and water (100 ml). The organic layer was dried over anhydrous

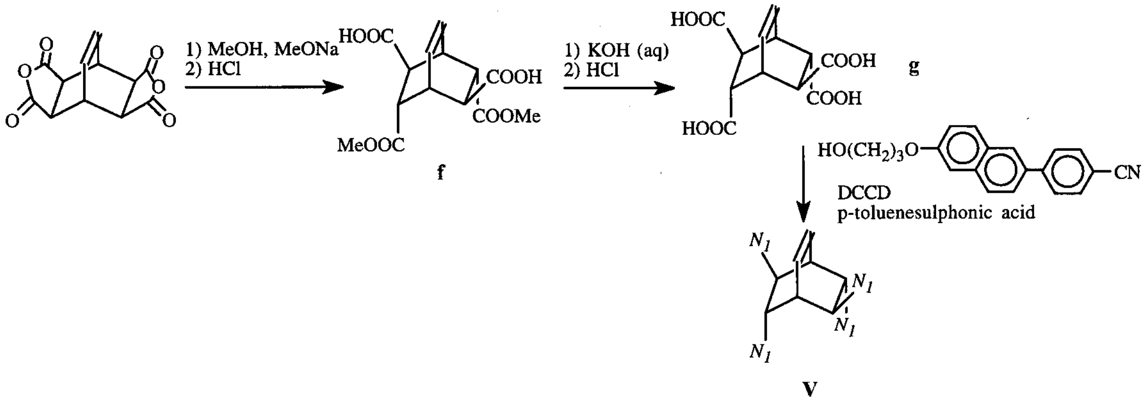

Scheme 3.

$MgSO_4$, and the volume reduced by evaporation. Upon column chromatography on silica gel using a gradient elution from CH_2Cl_2 to CH_2Cl_2:$(CH_3)_2CO$ (30:1), with subsequent precipitation into ethanol, compound **II** was obtained in 0.40 g (18%) yield; its structure was validated by elemental analysis and proton NMR spectroscopy.

2.2.7. *4-[(S)-(−)-1-Phenylethyl]-4-[(2-hydroxyethoxy)-benzoyloxy]benzamide (e)*

The synthesis and purification of this chiral precursor has been reported previously [20].

2.2.8. *Exo, exo-bicyclo[2.2.2]oct-7-ene-2,3,5,6-tetra-carboxylic acid, tetrakis{3-[6′-(4-cyanophenyl)-2′-naphthyloxy]-1-propyl ester} (**III**), and exo, exo-bicyclo[2.2.2]oct-7-ene-2,3,5,6-tetra-carboxlic acid, tris{3-[6′-(4-cyanophenyl)-2′-naphthyloxy]-1-propyl ester}, mono (S)-(−)-2-{4-[4-(1-phenyl-ethylcarbamoyl)-phenoxycarbonyl]phenoxy ethyl ester} (**IV**)*

Intermediate **b** (1.00 g, 3.30 mmol), intermediate **e** (0.45 g, 1.12 mmol), all *exo*-bicyclo-[2.2.2]oct-7-ene-2,3,5,6-tetracarboxylic acid (0.31 g, 1.10 mmol), and triphenylphosphine (1.21 g, 4.61 mmol) were added to anhydrous THF (20 ml) and anhydrous DMF (5 ml). Complete dissolution occurred upon addition of DEADC (0.76 ml, 4.8 mmol). The reaction mixture was stirred overnight, and its volume reduced by evaporation before precipitation with ethanol. The crude product was purified by column chromatography on silica gel with a gradient elution from CH_2Cl_2 to CH_2Cl_2:$(CH_3)_2CO$ (20:1) followed by precipitation with ethanol to yield compound **III** in 0.29 g (18%) yield and **IV** in 0.40 g (24%) yield; their structures were validated by elemental analysis and proton NMR spectroscopy.

2.2.9. *Bicyclo[2.2.2]oct-7-ene-(2,5)-exo-(3,6)-endo-tetracarboxylic acid, 3,6-dimethylester (f)*

Exo,exo-bicyclo[2.2.2]-7-ene-tetracarboxylic dianhydride (10.0 g, 40 mmol) and sodium methoxide (7.00 g, 130 mmol) were added to anhydrous methanol (150 ml). After heating under reflux overnight, the solvent was removed by evaporation before adding water (30 ml). The solution was kept below 4°C while acidifying with aqueous HCl (2M). The solid product was collected by filtration, yielding 3.5 g (28%), and its structure validated by proton NMR spectroscopy.

2.2.10. *Bicyclo[2.2.2]oct-7-ene-(2,5)-exo-(3,6)-endo-tetracarboxylic acid (g)*

Intermediate **f** (2.60 g, 8.3 mmol) was dissolved in NaOH solution (10%, 20 ml). After heating under reflux for 2 h, the reaction mixture was acidified with aqueous HCl (2M). The solid product was collected by filtration, yielding 1.0 g (42%), and its structure validated by elemental analysis and proton NMR spectroscopy.

2.2.11. *Bicyclo[2.2.2]oct-7-ene-2,5-exo-3,6-endo-tetra-carboxylic acid, tetrakis{3-[6′-(4-cyanophenyl)-2′-naphthyloxy]-1-propyl ester} (V)*

Intermediate **g** (0.15 g, 0.54 mmol), intermediate **b** (0.70 g, 2.31 mmol), dicyclohexylcarbodiimide, DCCD (0.54 g, 2.6 mmol) and *p*-toluenesulphonic acid (10 mg) were dissolved in pyridine (6 ml). The reaction mixture was stirred at room temperature overnight before adding acetic acid (1 ml) to consume excess DCCD. After filtering off solid residues, 50 ml water was added for acidification with aqueous HCl (2M). The resulting solid was dissolved in CH_2Cl_2 (100 ml) for extracting with $NaHCO_3$ solution (10%, 100 ml × 2) and water (100 ml × 2). The organic layer was dried over anhydrous $MgSO_4$. The crude product was purified by column chromatography on silica gel via a gradient elution from CH_2Cl_2:$(CH_3)_2CO$ (200:1) to (50:1), yielding compound **V** in 0.50 g (65%) yield; its structure was validated by elemental analysis and proton NMR spectroscopy.

2.2.12. *Bicyclo[2.2.2]oct-7-ene-2,5-exo-3,6-endo-tetracarboxylic acid, tetrakis{3,5-bis{3-[6′-(4-cyanophenyl)-2′-naphthyloxy]-1-propyloxycarbonyl}phenyl ester} (VI)*

Dry THF (25 ml) was added to intermediates **d** (1.00 g, 1.33 mmol) and **g** (0.092 g, 0.32 mmol), *p*-toluenesulphonic acid/4-dimethylaminiopyridine salt (0.10 g, 0.34 mmol) [23], and DCCD (0.31 g, 1.48 mmol). After stirring overnight, the insolubles were filtered off, and the filtrate was evaporated to dryness. The solid residue was shaken with CH_2Cl_2 (100 ml) and dilute acetic acid solution (100 ml). The organic layer was washed sequentially with water, saturated $NaHCO_3$ solution, water, and saturated NaCl solution (100 ml each) and then dried over anhydrous $MgSO_4$. The solution was then reduced to 25 ml in volume. After removing the insolubles, the crude product was purified by column chromatography on silica gel using CH_2Cl_2:$(CH_3)_2CO$ (30:1) as the eluent. Further purification was accomplished by precipitation into ethanol to yield compound **VI** in 0.84 g (78%) yield; its structure was validated by elemental analysis and proton NMR spectroscopy.

2.2.13. *1,3,5-Benzenetricarboxylic acid, tris{3-[6′-(4-cyanophenyl)-2′-naphthyloxy]-1-propyl ester} (VII)*

Benzene-1,3,5-tricarbonyl trichloride (0.28 g, 1.08 mmol), intermediate **b** (1.00 g, 3.3 mmol) and 4-dimethylaminopyridine (0.80 g, 6.6 mmol) were dissolved in 15 ml anhydrous THF. The solvent was removed by evaporation after 3 h reflux. The residue was dissolved in CH_2Cl_2 for washing sequentially with HCl solution (1M), $NaHCO_3$ solution (10%), and water. The organic layer was dried over anhydrous $MgSO_4$. Further purification was carried out by column chromatography on silica gel with CH_2Cl_2 as the eluent to yield compound **VII** in 0.80 g (73%) yield; its structure was validated by elemental analysis and proton NMR spectroscopy.

2.2.14. *1,3,5-Benzenetricarboxylic acid, tris{3,5-bis{3-[6′-(4-cyanophenyl)-2′-naphthyloxy]-1-propyloxycarbonyl}phenyl ester} (VIII)*

Intermediate **d** (0.50 g, 0.66 mmol), 1,3,5-benzenetricarbonyl chloride (0.055 g, 0.21 mmol) and 4-dimethylaminopyridine (0.16 g, 1.3 mmol) were dissolved in anhydrous THF (25 ml). After heating at reflux for 3 h, the reaction mixture was poured into water (70 ml). The solid was collected by filtration for column chromatography on silica using a gradient elution from CH_2Cl_2 to CH_2Cl_2:$(CH_3)_2CO$ (25:1). Compound **VIII** was obtained in 0.30 g (59%) yield; its structure was validated by elemental analysis and proton NMR spectroscopy.

2.3. *Characterization techniques*

2.3.1. *Molecular structures, thermotropic properties and morphology*

Chemical structures were determined with elemental analysis (performed by Oneida Research Services, Whitesboro, NY), and FTIR (Nicolet 20 SXC) and proton NMR (Avance-400, Bruker, and QE-300, GE) spectroscopic techniques. Thermal transition temperatures were determined by DSC (Perkin-Elmer DSC-7) with a continuous N_2 purge at 20 ml min^{-1}. Samples were preheated to 250°C followed by cooling at -20°C min^{-1} to -30°C before taking the reported heating scans at 20°C min^{-1}. The reported values of T_g and T_c were reproducible to within ±1°C. Liquid crystal mesomorphism was characterized with a polarizing optical microscope (Leitz Orthoplan-Pol) equipped with a hot stage (FP82, Mettler) and a central processor (FP80, Mettler); the nematic and cholesteric mesomorphism were identified by their threaded textures and oily streaks, respectively. The morphology of as-prepared and thermally processed samples was analysed with X-ray diffractometry (XRD). XRD data were collected in reflection mode geometry using a Rigaku RU-300 Bragg–Brentano diffractometer equipped with a copper rotating anode, diffracted beam graphite monochromator tuned to CuK_α radiation, and scintillation detector. Samples were analysed in powder form (as received), and as films (powders heated above T_c then cooled to 25°C at a rate of -20°C min^{-1}). All XRD data collection was carried out at 25°C.

2.3.2. *Measurements of order parameter and selective reflection on gLC films*

Optical elements for order parameter measurements were fabricated using optically flat, calcium fluoride substrates (1.00 in diameter × 0.04 in thick, Optovac) transparent in the infrared region. Optical elements for selective reflection measurements were made using optically flat, fused silica substrates (1.00 in diameter × 1/8 in thick, Esco Products) transparent to 200 nm. In both cases, the substrates were cleaned, spin-coated with Nylon 66, and then buffed with a velvet roller. Vitrified films were prepared by melting as-prepared powders between two surface-treated substrates at temperatures slightly above T_c and thermally annealed at temperatures slightly below T_c for 1 h before cooling at -30°C h^{-1} to room temperature. Thickness was controlled using glass fibre spacers (EM Industries) for the 14 μm films, and glass spheres (Bangs Laboratories) for the 2 μm films.

Order parameter was measured by linear dichroism using a FTIR spectrometer (Nicolet 20 SXC). Two measurements were performed with the transmission axis parallel and perpendicular to the nematic director (i.e. the buffing direction) of the sample. A UV-Vis-NIR spectrophotometer (Perkin-Elmer Lambda 9) was employed to measure light absorption (at normal incidence) and selective reflection (at 15° incidence from the surface normal) at room temperature. An aluminum mirror served as a specular reflection standard. The results were reported as % reflectivity of incident unpolarized light. In both the light absorption and light reflection measurements, Fresnel reflections from the two air–glass interfaces were accounted for using a reference cell comprising an index-matching fluid sandwiched between two surface-treated substrates.

Table 1. Elemental analysis of Compounds **I**–**VIII**.

Compound		C/%	H/%	N/%
I	calcd	77.29	5.36	3.92
	obsd	76.90	5.42	3.81
II	calcd	75.92	4.75	3.47
	obsd	75.87	4.88	3.50
III	calcd	77.51	5.09	3.93
	obsd	77.37	4.83	4.17
IV	calcd	75.48	5.15	3.67
	obsd	74.88	5.27	3.60
V	calcd	77.51	5.09	3.93
	obsd	77.21	5.29	3.84
VI	calcd	76.01	4.63	3.48
	obsd	75.62	4.81	3.61
VII	calcd	77.73	4.82	3.94
	obsd	77.29	4.86	3.85
VIII	calcd	76.11	4.51	3.48
	obsd	76.03	4.62	3.53

3. Results and discussion

The molecular structures of the high T_g gLCs depicted in figure 1 were elucidated with elemental analysis (see table 1) and proton NMR spectral data in $CDCl_3$ (see table 2). The equatorial configuration on the *cis,cis*-cyclohexane ring in compounds **I** and **II** was determined on the basis of NMR signals in the region between δ 1.50 and 3.00 [19]. The *exo,exo*-configuration on the bicyclo[2.2.2]oct-7-ene ring in **III** and **IV** was validated with signals near δ 3.10 and 3.40 attributed to the tertiary

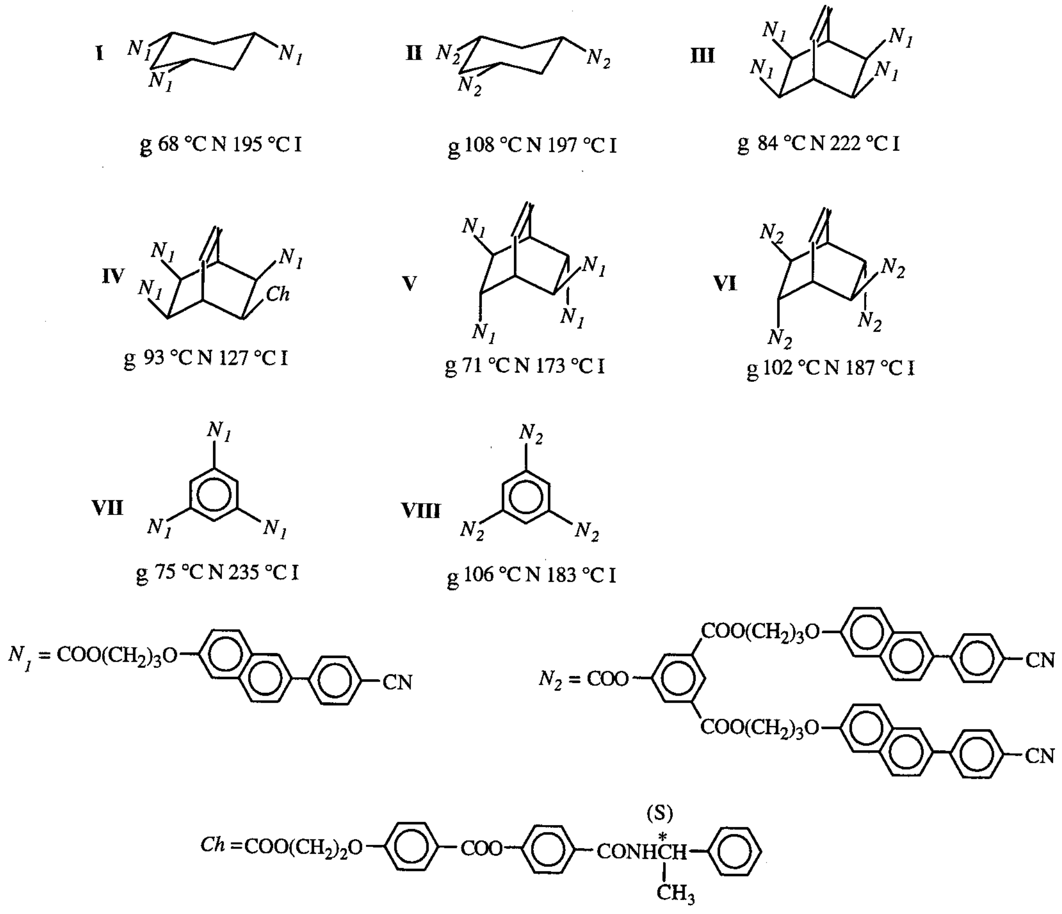

Figure 1. Molecular structures of glass-forming liquid crystals synthesized for the present study.

Table 2. Proton NMR (400 MHz) spectral data in $\mathrm{CDCl_3}$.

Compound	δ/ppm	Analysis
I	8.02–7.11	[m, 30 *H*, aromatic]
	4.35	[t, 6 *H*, $\mathrm{COOC}H_2\mathrm{CH}_2$, equatorial]
	4.16	[t, 6 *H*, $\mathrm{CH_2C}H_2\mathrm{O}$]
	2.67–2.23	[m, 6 *H*, *cis*-cyclohexane ring]
	2.19	[m, 6 *H*, $\mathrm{CH_2C}H_2\mathrm{CH_2}$]
	1.70–1.50	[m, 3 *H*, *cis*-cyclohexane ring]
II	8.63–7.11	[m, 69 *H*, aromatic]
	4.62	[t, 12 *H*, $\mathrm{COOC}H_2\mathrm{CH}_2$]
	4.23	[t, 12 *H*, $\mathrm{CH_2C}H_2\mathrm{O}$]
	2.92–2.63	[m, 6 *H*, *cis*-cyclohexane ring]
	2.34	[m, 6 *H*, $\mathrm{CH_2C}H_2\mathrm{CH_2}$]
	1.80–1.98	[m, 3 *H*, *cis*-cyclohexane ring]
III	7.98–7.04	[m, 40 *H*, aromatic}
	6.40	[m, 2 *H*, olefinic]
	4.33–4.12	[m, 8 *H*, $\mathrm{COOC}H_2\mathrm{CH}_2$, exo]
	4.04	[t, 8 *H*, $\mathrm{CH_2C}H_2\mathrm{O}$]
	3.39	[m, 2 *H*, C*H*, bridgehead]
	3.11	[s, 4 *H*, C*H*, tertiary]
	2.09	[m, 8 *H*, $\mathrm{CH_2C}H_2\mathrm{CH_2}$]
IV	8.12–6.84	[m, 43 *H*, aromatic]
	6.48–6.33	[m, 3 *H*, olefinic and CON*H*]
	5.38	[m, 1 *H*, $\mathrm{NHC}H(\mathrm{CH_3})$]
	4.44–3.99	[m, 16 *H*, $\mathrm{COOC}H_2\mathrm{CH_2C}H_2\mathrm{O}$ and $\mathrm{COOC}H_2\mathrm{C}H_2\mathrm{O}$]
	3.41	[d, 2 *H*, C*H*, bridgehead]
	3.13	[d, 4 *H*, C*H*, tertiary]
	2.12	[m, 6 *H*, $\mathrm{CH_2C}H_2\mathrm{CH_2}$]
	1.63	[d, 3 *H*, $\mathrm{CH(C}H_3)$]
V	7.98–7.04	[m, 40 *H*, aromatic]
	6.31	[m, 2 *H*, olefinic]
	4.35	[m, 4 *H*, $\mathrm{COOC}H_2\mathrm{CH}_2$, *endo*]
	4.23	[m, 4 *H*, $\mathrm{COOC}H_2\mathrm{CH}_2$, *exo*]
	4.07	[t, 4 *H*, $\mathrm{CH_2C}H_2\mathrm{O}$, *endo*]
	4.00	[t, 4 *H*, $\mathrm{CH_2C}H_2\mathrm{O}$ *exo*]
	3.57	[m, 2 *H*, C*H*, bridgehead]
	3.28	[m, 2 *H*, C*H*, tertiary, *endo*]
	3.02	[m, 2 *H*, C*H*, tertiary, *exo*]
	2.15	[m, 4 *H*, $\mathrm{CH_2C}H_2\mathrm{CH_2}$, *endo*]
	2.05	[m, 4 *H*, $\mathrm{CH_2C}H_2\mathrm{CH_2}$, *exo*]
VI	8.66–7.04	[m, 92 *H*, aromatic]
	6.51	[m, 2 *H*, olefinic]
	4.62–4.40	[m, 16 *H*, $\mathrm{COOC}H_2\mathrm{CH}_2$, *endo* and *exo*]
	4.35–4.16	[m, 16 *H*, $\mathrm{CH_2C}H_2\mathrm{O}$ *endo* and *exo*]
	4.10	[m 2 *H*, C*H*, bridgehead]
	3.86	[m, 2 *H*, C*H*, tertiary, *endo*]
	3.55	[m, 2 *H*, C*H*, tertiary, *exo*]
	2.40–2.10	[m, 16 *H*, $\mathrm{CH_2C}H_2\mathrm{CH_2}$, *endo* and *exo*]
VII	8.90–7.11	[m, 33 *H*, aromatic]
	4.70	[t, 6 *H*, $\mathrm{COOC}H_2\mathrm{CH}_2$]
	4.26	[t, 6 *H*, $\mathrm{CH_2C}H_2\mathrm{O}$]
	2.30	[m, 6 *H*, $\mathrm{CH_2C}H_2\mathrm{CH_2}$]
VIII	9.52–7.11	[m, 72 *H*, aromatic]
	4.66	[t, 12 *H*, $\mathrm{COOC}H_2\mathrm{CH}_2$]
	4.28	[t, 12 *H*, $\mathrm{CH_2C}H_2\mathrm{O}$]
	2.39	[m, 12 *H*, $\mathrm{CH_2C}H_2\mathrm{CH_2}$]

(*endo*-) and bridgehead protons, respectively [24]. Note the two triplets at δ 4.35 and 4.16, attributable to the trimethylene spacer in **I**, emerge as a multiplet at δ 4.21 and a triplet at δ 4.04 in **III**, presumably because of the hindered rotation by the N_1 pendants constrained on an *exo*,*exo*-bicyclo-octene ring. The singlet at δ 3.11 attributable to the tertiary protons in **III** with an *exo*,*exo*-configuration is split into two multiplets at

δ 3.02 (*exo*-protons) and δ 3.28 (*endo*-protons) with equal intensities in the *exo,endo*-configuration of **V** [25]. The signal attributable to the bridgehead proton was found to undergo a downfield shift to δ 3.57 in **V** from δ 3.39 in **III**. It appears that the nematic pendants on the *exo,endo*-bicyclo-octene ring in **V** are subject to hindered rotation, as in the *exo,exo*-configuration of **III**. In addition, the *endo*- and *exo*-oriented, trimethylene spacer yielded distinct signals. Therefore, the two multiplets at δ 2.09 and 4.21 plus the triplet at δ 4.04 in **III** split into two sets of multiplets (2.05, 2.15) and (4.23, 4.35) plus one set of triplets (4.00, 4.07) in **V**. In each set the higher field signal is attributed to the *exo*-configuration, and the lower to the *endo*-configuration in the *exo,endo*-bicyclo-octene ring [26]. The signals associated with the trimethylene spacer in **VI** are similar to those found in **V** except for the partial overlap of signals from the *endo*- and *exo*-configuration. In the case of the benzene core, free rotation of both the N_1 and N_2 pendants seems to prevail based on the NMR signals attributable to the trimethylene spacer in **VII** and **VIII**, the two triplets near δ 4.70 and 4.26 as shown in table 2.

For a consistent evaluation of thermal transition temperatures by DSC, all as-prepared samples were heated beyond the clearing temperature, T_c, and then cooled at -20°C min^{-1} to -30°C before taking a heating scan at 20°C min^{-1}. The resultant thermograms were used to determine T_g and T_c with the nematic and chiral-nematic (i.e. cholesteric) mesophase identified by threaded textures and oily streaks, respectively, under polarizing optical microscopy. The nematic gLCs, **I–VII**, except **IV**, were further characterized by linear dichroism associated with the C≡N bond stretching at 2225 cm^{-1}, as shown in figure 2, where absorbances parallel ($A_\parallel$) and perpendicular ($A_\perp$) to the nematic director are shown. With the dichroic ratio, $R = A_\parallel / A_\perp$, the orientational order parameter can be determined, $S = (R - 1)/(R + 2)$, assuming that the absorption transition moment is parallel to the nematic director. The thermotropic transition temperature, the heat capacity change accompanying glass transition, the enthalpy of clearing (i.e. nematic or chiral-nematic to isotropic transition), and the order parameter are presented in table 3.

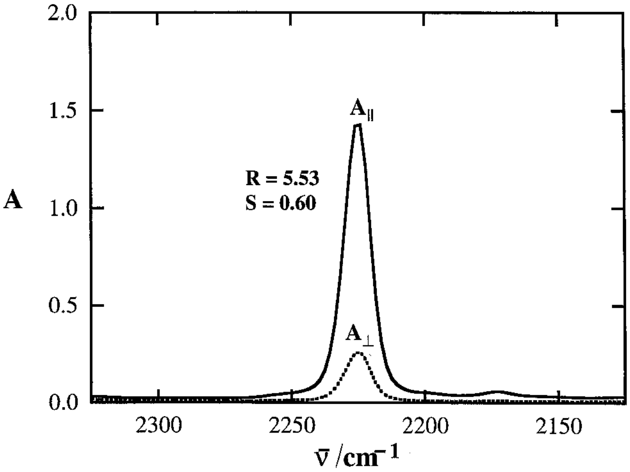

Figure 2. FTIR linear dichroism of C≡N bond stretching at 2225 cm^{-1}, measured for a nematic gLC film prepared with compound **VIII**: $A_\parallel$ and $A_\perp$ are absorbances parallel and perpendicular to the nematic director, respectively; dichroic ratio $R = A_\parallel / A_\perp$, and the orientational order parameter $S = (R - 1)/(R + 2)$.

Table 3. Thermotropic properties and order parameters of compounds **I–VIII**.

Compound	Transition temperatures/°C[a]	Order parameter, S[b]
I	g 68(0.29) N 195(1.80) I	0.63
II	g 108(0.18) N 197(2.14) I	0.59
III	g 84(0.28) N 222(2.51) I	0.52
IV	g 93(0.29) Ch 127(0.55) I	—
V	g 71(0.28) N 173(1.20) I	0.52
VI	g 102(0.16) N 187(1.19) I	0.59
VII	g 75(0.24) N 235(1.72) I	0.56
VIII	g 106(0.24) N 183(2.09) I	0.60

[a] Symbols: g glassy; N nematic; Ch chiral nematic; I isotropic. The numbers following G, N, and Ch are glass, nematic-to-isotropic, and chiral-nematic to isotropic transition temperatures, respectively. The numbers in parentheses following g denote heat capacity change in J g^{-1} °C^{-1} accompanying glass transition, and those following N and Ch denote enthalpy of clearing in J g^{-1}.

[b] Orientational order parameter measured for 14 µm thick nematic gLC films with FTIR linear dichroism.

To unravel the effects of structural parameters on phase transition temperatures, the nematic precursors were also characterized with DSC heating scans at 20°C min^{-1} of samples preheated to 250°C. A T_m of 132°C and a T_c of 196°C were found for 2-(3′-hydroxy-1′-propyloxy)-6-(4-cyanophenyl)naphthalene. In contrast, a T_m of 221°C and a T_c of 251°C were found for 1-hydroxy-3,5-benzenedicarboxylic acid bis{3-[6′-(4-cyanophenyl)-2′-naphthyloxy]-1-propyl ester}. Therefore, N_2 appears to be a stronger nematogen than N_1. Moreover, in comparison with N_1, N_2 affords not only an extended central core from the *cis,cis*-cyclohexane base but also an increased number of pendants from 3 to 6 per gLC molecule. All three factors contribute to an elevation in T_g of **II** over **I** by 40°C. Similarly, **VI** and **VIII** show an elevation in T_g by 31°C over **V** and **VII**, respectively. However, no consistent trend in T_c seems to result from extending the central core. For a given nematic pendant, N_1 or N_2, T_g seems to be relatively insensitive to the central core structure, be it *cis,cis*-cyclohexane, *exo,endo*-bicyclo-octene, or benzene. None the less, a configuration modification from *exo,endo*- to *exo,exo*-bicyclo-octene results in an elevation in T_g by 13°C and in T_c by 49°C, **III** vs. **V**.

As a co-product from the statistical reaction conducted for compound **III**, compound **IV** was obtained as a chiral-nematic gLC with a T_g of 93°C and a T_c of 127°C, representing an elevation in T_g by 10 to 20°C over all the chiral-nematics reported previously [20, 26]. Specifically, there are three nematic and one chiral pendants in compound **IV**, as opposed to two nematic and one chiral pendants in the cyclohexane-based chiral-nematic gLCs [20, 26]. It is noted that the replacement of one of the nematic pendants in **III** with a non-mesogenic, chiral pendant produces a chiral-nematic gLC with a somewhat elevated T_g but a much depressed T_c. Compound **IV** was melt-processed into a 2 μm thick gLC film, labelled as A in figure 3, yielding a selective reflection band around 375 nm. With an aluminum mirror serving as a specular reflector for incident unpolarized light, a perfect chiral-nematic film would yield a reflectivity of 50%. Since selective reflection appears in the UV region, it is important to assess the extent to which light absorption distorts selective reflection. Since the chiral pendant absorbs light at a shorter wavelength than the nematic pendant, UV absorption was measured for compound **III** in methylene chloride at 10^{-5} M. The result is presented as D in figure 3 in terms of extinction coefficient, indicating that part of the selective reflection band of the film prepared with **IV** is indeed lost to the absorption of incident light in the reflection measurement. The selective reflection spectra of 2 μm thick gLC films prepared with mixtures at molar ratios **IV**:**III** = 78:21 and 49:51 are presented as B and C, respectively, in figure 3. As expected, the selective reflection band undergoes a bathochromic shift at a decreasing chiral content. Film B was further used to demonstrate that (*S*)-(−)-1-phenylethylamine gives rise to a left-handed chiral-nematic film based on the handedness of reflected incident light [27].

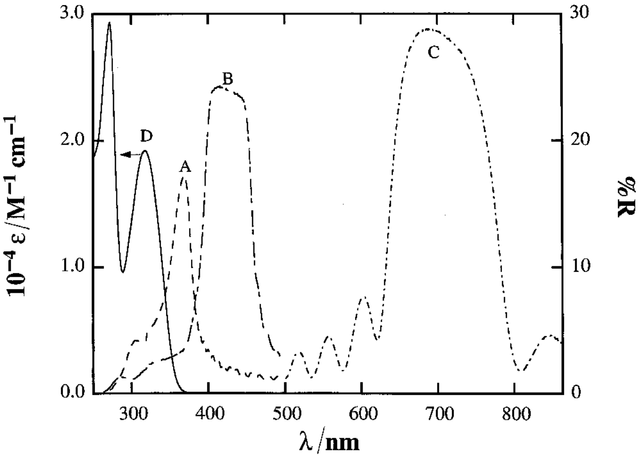

Figure 3. Reflectivity measured with unpolarized light incident on 2 μm thick chiral-nematic gLC films with the following **IV**:**III** molar ratios: A 100:0; B 78:22; C 49:51. Extinction coefficient of nematic pendant is shown as D measured with **III** in methylene chloride at 10^{-5} M concentration.

Finally, the morphology of as-prepared samples and that of thermally processed gLCs were characterized by X-ray diffractometry at room temperature. As illustrated in figure 4, the as-prepared powders of **VIII** are non-crystalline. Moreover, heating as-prepared samples to beyond T_c with subsequent thermal annealing at temperatures slightly below T_c for up to 1 h before cooling to room temperature produced nematic gLCs that remain non-crystalline when left at room temperature for six months as illustrated with compound **VIII** in figure 4.

4. Summary

A strategy to elevate the T_g of glass-forming liquid crystals was implemented by increasing the volume of the non-mesogenic central core with an attendant increase in the number of mesogenic pendants per gLC

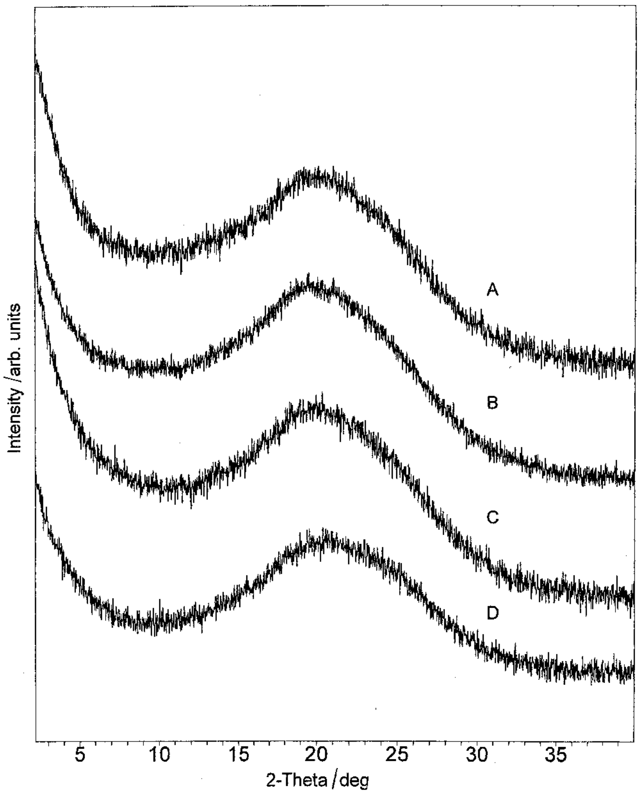

Figure 4. X-ray diffraction patterns of compound **VIII**: A as-prepared sample; B immediately upon thermal processing (i.e. heating as-prepared sample to beyond T_c, thermal annealing at a temperature slightly below T_c and then cooling to room temperature); C two months afterwards; D six months afterwards.

molecule. The concept was demonstrated with new gLCs possessing a T_g above 100°C with the following key observations:

(i) An extended central core accompanied by an increased number of nematic pendants over the benzene, *cis*,*cis*-cyclohexane, and *exo*,*endo*-bicyclo-[2.2.2]oct-7-ene base structures was found to elevate T_g by 30 to 40°C without a definite trend in T_c.

(ii) The *exo*,*endo*-bicyclo[2.2.2]oct-7-ene central core was prepared via modification of the *exo*,*exo*-configuration with its stereochemistry validated by proton NMR spectroscopy. With the same nematic pendant, the *exo*,*exo*-GLC showed an elevation in T_g by 13°C and in T_c by 49°C over the *exo*,*endo*-counterpart.

(iii) A left-handed chiral-nematic gLC emerged from (*S*)-(−)-1-phenylethylamine as the chiral moiety. Selective reflection bands ranging from the UV to the visible spectral region were demonstrated with gLC films at a decreasing chiral content.

(iv) Heating as-prepared samples to beyond T_c followed by thermal annealing at temperatures slightly below T_c and then cooling to room temperature produced well aligned nematic gLC films as quantified by the orientational order parameter measured with FTIR linear dichroism.

(v) X-ray diffraction patterns revealed the non-crystalline morphology of all as-prepared samples. Thermally processed gLC samples were found to remain non-crystalline when left at room temperature for six months.

The authors wish to express their gratitude to S. D. Jacobs, K. L. Marshall, and A. W. Schmid of the Laboratory for Laser Energetics (LLE), A. S. Kende of the Department of Chemistry at the University of Rochester, and P. J. Hood of Cornerstone Research Group, Inc., Dayton Ohio for their technical advice and helpful discussions. The funding of this work was provided by the National Science Foundation under Grants CTS-9811172, CTS-9818234, and CHE-9120001. Additional support was provided by the Air Force Office of Scientific Research under Contract F49620-98-C-0060, the Department of Energy Office of Inertial Confinement Fusion under Cooperative Agreement No. DE-FC03-92SF19460 with LLE, and the New York State Energy Research and Development Authority. The support of DOE does not constitute an endorsement by DOE of the views expressed in this article.

References

[1] Collings, P. J., and Patel, J. S., 1997, *Handbook of Liquid Crystal Research* (New York: Oxford University Press).
[2] Wedler, W., Demus, D., Zaschke, H., Mohr, K., Schäfer, W., and Weissflog, W., 1991, *J. mater. Chem.*, **1,** 347.
[3] Attard, G. S., Imrie, C. T., and Karasz, F. E., 1992, *Chem. Mater.*, **4,** 1246.
[4] Neumann, B., Joachimi, D., and Tschierske, C., 1997, *Adv. Mater.*, **9,** 241.
[5] Gresham, K. D., McHugh, C. M., Bunning, T. J., Crane, R. L., Klei, H. E., and Samulski, E. T., 1994, *J. polym. Sci. A*, **32,** 2039.
[6] Ortler, R., Braucle, C., Miller, A., and Riepl, G., 1989, *Macromol. Chem., rapid Commun.*, **10,** 189.
[7] Tamaoki, N., Parfenov, A. V., Masaki, A., and Matsuda, H., 1997, *Adv. Mater.*, **9,** 1102.
[8] Wang, H., Jin, M. Y., Jarnagin, R. C., Bunning, T. J., Adams, W., Cull, B., Shi, Y., Kumar, S., and Samulski, E. T., 1996, *Nature*, **384,** 244.
[9] Loddoch, M., Marowsky, G., Schmid, H., and Heppke, G., 1994, *Appl. Phys. B*, **59,** 591.
[10] Natarajan, L. V., Bunning, T. J., Klei, H. E., Crane, R. L., and Adams, W. W., 1991, *Macromolecules*, **24,** 6554.
[11] Morita, Y., Stockley, J. E., Johnson, K. M., Hanelt, E., and Sandmeyer, F., 1999, *Jpn. J. appl. Phys.*, **38,** 95.
[12] Van de Witte, P., and Lub, J., 1999, *Liq. Cryst.*, **26,** 1039.
[13] Chen, S. H., Shi, H., Conger, B. M., Mastrangelo, J. C., and Tsutsui, T., 1996, *Adv. Mater.*, **8,** 998.
[14] Chen, S. H., Mastrangelo, J. C., Shi, H., Bashir-Hashemi, A., Li, J., and Gelber, N., 1995, *Macromolecules*, **28,** 7775.
[15] Chen, S. H., Mastrangelo, J. C., Shi, H., Blanton, T. N., and Bashir-Hashemi, A., 1997, *Macromolecules*, **30,** 93.
[16] Chen, S. H., Mastrangelo, J. C., Blanton, T. N., Bashir-Hashemi, A., and Marshall, K. L., 1997, *Liq. Cryst.*, **21,** 683.
[17] Shi, H., Chen, S. H., de Rosa, M. E., Bunning, T. J., and Adams, W. W., 1996, *Liq. Cryst.*, **20,** 277.
[18] Shi, H., Katsis, D., Chen, S. H., DeRosa, M. E., Adams, W. W., and Bunning, T. J., 1996, *Mat. Res. Soc, Symp. Proc.*, **425,** 27.
[19] Shi, H., and Chen, S. H., 1995, *Liq. Cryst.*, **19,** 785.
[20] Katsis, D., Chen, P. H. M., Mastrangelo, J. C., Chen, S. H., and Blanton, T. N., 1999, *Chem. Mater.*, **11,** 1590.
[21] Chen, S. H., Katsis, D., Schmid, A. W., Mastrangelo, J. C., Tsutsui, T., and Blanton, T. N., 1999, *Nature*, **397,** 506.
[22] Collington, E. W., Finch, H., and Smith, I. J., 1985, *Tetrahedron Lett.*, **26,** 681.
[23] Moore, J. S., and Stupp, S. I., 1990, *Macromolecules*, **23,** 65.
[24] Mastrangelo, J. C., Chen, S. H., and Blanton, T. N., 1995, *Chem. Mater.*, **7,** 1904.
[25] Iordache, F., Chiraleu, F., and Avram, M., 1975, *Rev., Roum. Chim.*, **20,** 233.
[26] Shi, H., and Chen, S. H., 1995, *Liq. Cryst.*, **19,** 849.
[27] Chen, S. H., Katsis, D., Chen, P. H., Mastrangelo, J. C., and Tsutsui, T., 1999, *Polym. Prepr.*, **40,** 1171.